Am J Transl Res 2025;17(3):2145-2153
www.ajtr.org /ISSN:1943-8141/AJTR0160677

Original Article

Cirsiliol suppresses malignant progression of hepatocellular carcinoma via regulation of glutamine metabolism

Bin Zhang, Jianbo Zheng, Siming Zheng

Hepatopancreatobiliary Surgery Department, The First Affiliated Hospital of Ningbo University, No. 59, Liuting Street, Haishu District, Ningbo 315000, Zhejiang, China

Received September 22, 2024; Accepted December 6, 2024; Epub March 15, 2025; Published March 30, 2025

Abstract: Background: To investigate the therapeutic potential of cirsiliol in hepatocellular carcinoma (HCC), focusing on its impact on glutamine metabolism. Methods: HCC cell lines HCCLM3 and Huh7 were treated with cirsiliol, and cell viability and proliferation were assessed using CCK-8 assay. Intracellular concentrations of glutamine, α-ketoglutaric acid (α-KG), and adenosine triphosphate (ATP) were measured to evaluate glutamine metabolism. A xenograft tumor model was employed to examine the in vivo effects of cirsiliol. Additionally, network pharmacological analysis was used to identify potential targets of cirsiliol in HCC. Western blotting was conducted to analyze the modulation of the PI3K/AKT signaling pathway by cirsiliol. Results: Cirsiliol significantly inhibited HCC cell growth both in vitro and in vivo while reducing levels of glutamine, α-KG, and ATP, indicating suppression of glutamine metabolism. Activation of the PI3K signaling pathway reversed the inhibitory effects of cirsiliol on HCC cell growth and metabolism. Conclusion: Cirsiliol suppresses glutamine metabolism and inhibits the growth of HCC cells by modulating the PI3K/AKT signaling pathway.

Keywords: Hepatocellular carcinoma, cirsiliol, glutamine metabolism, PI3K

Introduction

Cancer cells undergo metabolic reprogramming to adapt their metabolic processes, ensuring sufficient energy supply, building blocks for biosynthesis, redox balance, and rapid cell division [1, 2]. A hallmark of this reprogramming is dysregulated glucose metabolism, commonly observed in many cancers. Cancer cells exhibit increased glucose uptake compared to normal cells, with the majority of glucose converted into lactate and secreted, bypassing the tricarboxylic acid (TCA) cycle, a phenomenon known as the Warburg effect [3]. Consequently, in rapidly proliferating cancer cells, this altered glucose metabolism often fails to produce adequate ATP or intermediates for anabolic processes [4].

Glutamine, the most abundant amino acid in mammals, serves as an alternative energy source. Cancer cells exhibit an increased dependency on glutamine, enhancing its turnover to meet bioenergetic and biosynthetic demands for sustained growth [5]. This reliance on glutamine metabolism is a strategic adaptation to support rapid proliferation. Glutamine is transported into cells via the alanine-serine-cysteine transporter 2 (ASCT2) and catabolized to glutamate in the mitochondria by glutaminase (GLS) [6]. Glutamate is then converted into α-KG, primarily by glutamate dehydrogenase 1 (GLUD1), a critical step for fueling the TCA cycle and ATP production [7]. Furthermore, glutamine serves as a nitrogen donor for nucleotide and amino acid synthesis, essential for DNA replication and protein production. Additionally, it contributes to the synthesis of glutathione, a tripeptide vital for protecting cells against oxidative stress and maintaining redox balance [8, 9].

Cirsiliol, a natural flavonoid extracted from plants, is recognized for its diverse biological activities, particularly its anti-tumor effects, which have attracted significant research attention [10-12]. For example, cirsiliol inhibits

https://doi.org/10.62347/AOTY4308

the proliferation of methotrexate-resistant osteosarcoma cells and induces apoptosis by targeting the AKT pathway. This action reduces AKT phosphorylation, thereby enhancing the transcriptional activity of the forkhead box O transcription factor 1 (FOXO1) [13]. Additionally, cirsiliol inhibits TYK2 kinase activity, leading to decreased phosphorylation of the substrate protein STAT3. This reduction diminishes STAT3 nuclear translocation and the transcription of downstream oncoproteins [14]. These findings highlight cirsiliol's potential as an anti-tumor agent. However, its role in hepatocellular carcinoma (HCC) remains unclear, and its involvement in aberrant glutamine metabolism in cancer has not been elucidated. This study aimed to investigate the effects of cirsiliol on HCC growth and glutamine metabolism.

Materials and methods

Cell culture

The HCC cell lines HCCLM3 and Huh7 were obtained from the Cell Bank of the Committee on Type Culture Collection, Chinese Academy of Sciences. Cells were cultured in high-glucose Dulbecco's Modified Eagle Medium (DMEM; Gibco), supplemented with 10% fetal bovine serum (FBS), at 37°C in a humidified incubator with 5% CO_2. For in vitro experiments, cirsiliol (HY-110399, MCE, USA) and the PI3K activator 740Y-P (HY-P0175, MCE, USA) were administered at concentrations of 20 μM and 15 μM, respectively, in the culture medium for the indicated durations or 24 hours.

Cell viability

Cell viability and proliferation were evaluated using the Cell Counting Kit-8 (CCK-8; Solarbio, China) and the Cell-Light EdU Apollo567 In Vitro Kit (RiboBio, China), following the manufacturers' instructions. For the CCK-8 assay, 10,000 cells per well were seeded in 96-well plates and cultured in high-glucose DMEM with 10% FBS for the specified time. Afterward, 10 μL of CCK-8 reagent was added to each well, and the plates were incubated for 2 hours. Optical density (OD) at 450 nm was measured using a microplate reader (Model 680, Bio-Rad). For the EdU (5-ethynyl-2'-deoxyuridine) assay, cells were seeded into 96-well plates, fixed, and incubated with EdU reagent for 30 minutes. The cells were then permeabilized and stained with Apollo567 dye. Fluorescence images were captured using a fluorescence microscope (Leica, Germany).

Animal experiments

Animal studies were approved by the Animal Care and Use Committee of The First Affiliated Hospital of Ningbo University. Male BALB/c nu/nu mice, six weeks old and weighing approximately 18 g, were randomly assigned to groups before inoculation. The mice were housed in a standard laboratory environment with free access to food and water, under a 12-hour light/dark cycle. All procedures were conducted under sterile conditions.

To establish subcutaneous tumor models, 5×10^6 HCCLM3 cells suspended in 100 μL of phosphate-buffered saline (PBS) were injected subcutaneously into the flanks of the mice. Tumor size was measured using a digital caliper, and volume was calculated as: tumor volume = (length × width^2)/2. When tumor volumes reached approximately 100 mm^3 (about 7 days after inoculation), mice were randomized into experimental groups (n=5 per group) and received oral administration of cirsiliol (20 mg/kg body weight) or PBS (control group) every three days for 18 days. At the end of the experiment, mice were euthanized by cervical dislocation, and tumor tissues were collected for imaging and further analysis.

Glutamine metabolism

The glutamine metabolism was assessed by measuring intracellular levels of glutamine, ATP, and α-ketoglutaric acid (α-KG). Glutamine uptake, consumption rates, and glutamate production were quantified using the Glutamine Assay Kit (Abnova, Catalog No. KA1627) and Glutamate Assay Kit (Sigma, Catalog No. MAK004-1KT), following the manufacturers' protocols.

For ATP measurement, cells grown in 24-well plates were washed with 500 μL of PBS and lysed using 250 μL of lysis reagent designed for luciferase assays (Promega, USA). Lysates were centrifuged at 13,000 g for 1 minute to separate cellular components. ATP content was quantified by mixing 50 μL of supernatant with 50 μL of CellTiter-Glo reagent, followed by 10 minutes of incubation in the dark. Luminescen-

ce was measured using a TECAN plate reader (China). For α-KG detection, the BC5425 α-KG Assay Kit (Sosarbio) was used according to the manufacturer's protocol.

RNA extraction and quantitative real time PCR (qRT-PCR) assay

Total RNA was extracted using TRIzol reagent (Life Technologies, USA) following the manufacturer's instructions. RNA concentration was measured at 260 nm using the ND-100 Nanodrop analyzer (Nanodrop Technologies, USA). Complementary DNA (cDNA) was synthesized from 1 μg of RNA using SuperScript II reverse transcriptase and an Oligo (dT) primer (Invitrogen, USA). A total of 25 ng of cDNA in a 10 μL reaction volume was subjected to qRT-PCR using SYBR Green qPCR Master Mix (Applied Biosystems). Reactions were performed in triplicate on the ABI 7500 Fast Real-Time PCR System. Gene expression levels were calculated using the ΔΔCT method, with β-actin serving as the internal control.

Western blot assay

Cells were lysed in SDS-containing buffer with protease inhibitors (Roche, USA) for 30 minutes, followed by heating at 100°C for 10 minutes to denature proteins. Protein concentrations were determined using the Bicinchoninic Acid (BCA) Assay Kit (Pierce, USA). For electrophoresis, 50 μg of protein per sample was resolved via SDS-PAGE and transferred onto PVDF membranes. Membranes were incubated overnight at 4°C with primary antibodies against PI3K (1:2000, PA5-99518, Thermo, USA) and p-PI3K (1:2000, PA5-17387, Thermo, USA). Secondary antibodies, anti-rabbit (1:5000, ab6721, Abcam, USA) or anti-mouse (1:5000, ab6728, Abcam, USA), were applied the next day. Immunoreactive bands were visualized using an ECL detection system (GE Healthcare Bioscience, USA) as per the manufacturer's guidelines.

Network pharmacological analysis

Effective drug components were retrieved from the TCMSP database using criteria of OB ≥ 30% (oral bioavailability) and DL ≥ 0.18 (drug-likeness). Targets were standardized and deduplicated using the UniProt database, and gene name abbreviations were obtained. Disease-associated targets were sourced from GeneCards, TTD, and OMIM databases, with duplicate entries removed. Venn diagrams identified intersecting targets between traditional Chinese medicine and disease-associated targets. Protein-protein interaction networks were constructed using the STRING database (species: Homo sapiens, default parameters) and visualized in Cytoscape. Key targets were identified using degree centrality. GO (BP, CC, MF), KEGG, HALLMARK, and REACTOME enrichment analyses were conducted using the R package clusterProfiler, with a q-value <0.05 indicating significance. The top pathways were visualized, and protein-protein interaction networks were further analyzed using the R package STRINGdb.

Statistical analysis

All statistical analyses were performed using GraphPad Prism 8.0 and SPSS 19.0. Differences between the two groups were analyzed using the Student's t-test, while one-way or two-way ANOVA was applied for comparisons among multiple groups. A *p*-value <0.05 was considered statistically significant.

Results

Cirsiliol represses HCC growth and glutamine metabolism in vitro

HCCLM3 and Huh7 cells were treated with cirsiliol at a concentration of 20 μM for 24 hours, followed by assessments of cell viability and glutamine metabolism. As shown in **Figure 1A** and **1B**, cirsiliol significantly inhibited cell proliferation and reduced the proportion of EdU-positive cells. Cirsiliol treatment also elevated intracellular glutamine levels (**Figure 1C**) while reducing levels of glutamic acid (**Figure 1D**), α-KG (**Figure 1E**), and ATP (**Figure 1F**).

Cirsiliol inhibits hcc growth in vivo

The effects of cirsiliol were further investigated using a xenograft tumor model. Administration of cirsiliol significantly suppressed tumor growth and reduced tumor size (**Figure 2A-C**). Consistent with the in vitro results, cirsiliol treatment increased glutamine levels in tumor tissues (**Figure 2D**) and decreased glutamic acid (**Figure 2E**) and α-KG levels (**Figure 2F**).

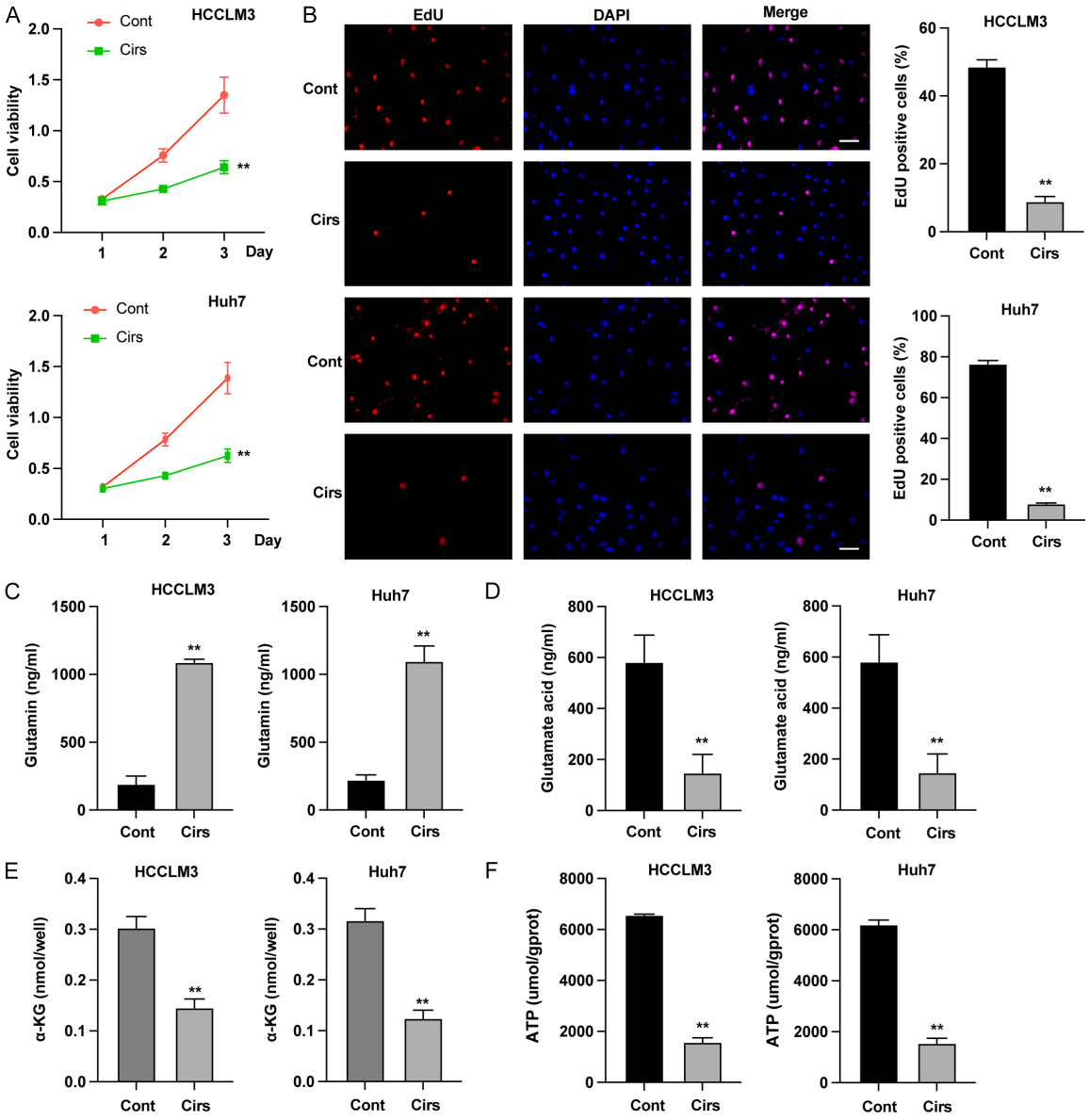

Figure 1. Cirsiliol suppresses the in vitro growth and glutamine metabolism of hepatocellular carcinoma. A: Cell viability was measured by CCK-8 assay. B: Cell proliferation was determined by EdU assay. Scale bar: 20 μm. C-F: The intracellular levels of glutamine, glutamic acid, α-ketoglutaric acid, and adenosine triphosphate. **P<0.05.

Network pharmacology analysis of cirsiliol's target pathways in HCC

The TCMSP database identified 10 target genes for cirsiliol, including NOS2, SCN5A, PTGS2, F7, DPP4, PYGM, HSP90AB1, PRSS1, NCOA2, and CALM1 (**Figure 3A**). Searches in the Genecard, TTD, and OMIM databases identified 3,559, 65, and 74 disease-associated targets, respectively (**Figure 3B**). Intersection analysis revealed 10 overlapping genes (**Figure 3C**). Enrichment analysis of these genes showed that cirsiliol targets cellular processes and signaling pathways associated with metabolism and oxygen response (**Figure 3D**, **3E**). Protein-protein interaction (PPI) network analysis (**Figure 3F**) and subsequent GO and KEGG enrichment analysis highlighted terms such as regulation of cell death, apoptotic processes, phosphorylation, and MAPK signaling (**Figure 3G**, **3H**).

Cirsiliol regulates glutamine metabolism in HCC through the PI3K signaling pathway

To explore how cirsiliol modulates glutamine metabolism in HCC cells, we investigated the

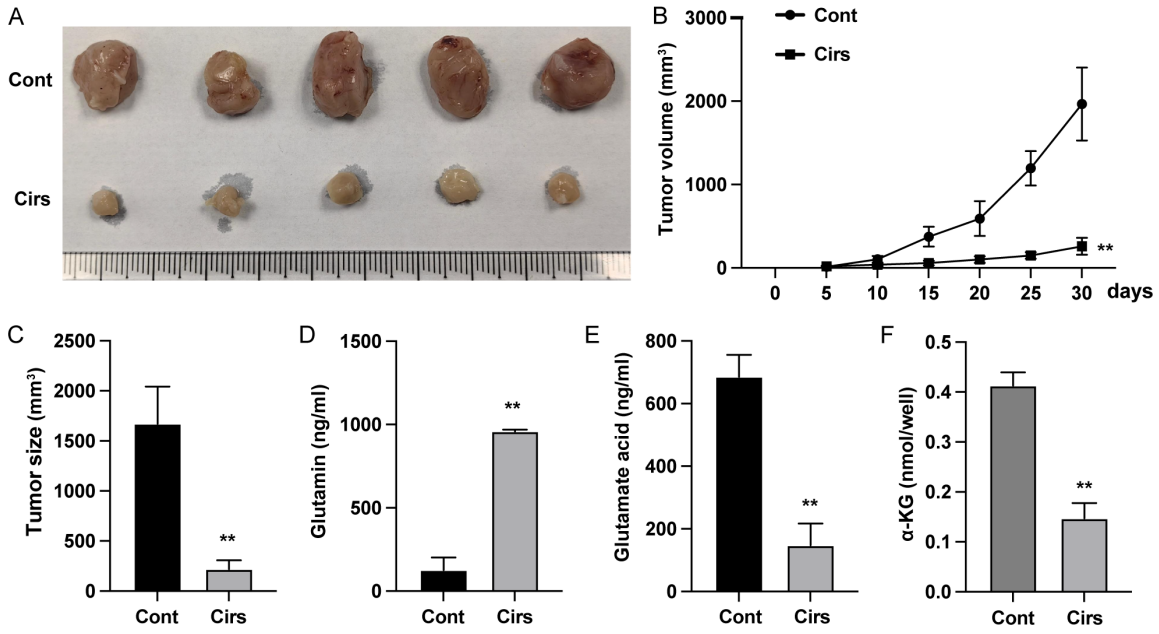

Figure 2. Cirsiliol inhibits the in vivo growth of hepatocellular carcinoma cells. An Ishikawa cell xenograft tumor model was established. A-C: Tumor growth curve and tumor size are presented. D-F: The levels of glutamine, glutamic acid, and α-ketoglutaric acid, in tumor tissues are shown. **P<0.05.

PI3K/AKT signaling pathway. HCC cells were exposed to a PI3K activator (740Y-P, 15 μM) and cirsiliol (20 μM) for 24 hours. The PI3K activator enhanced PI3K phosphorylation, an effect reversed by cirsiliol (**Figures 4A** and S1). Furthermore, the PI3K activator increased levels of glutamic acid (**Figure 4B**), α-KG (**Figure 4C**), and ATP (**Figure 4D**), suggesting a regulatory link between the PI3K/AKT pathway and cirsiliol-induced metabolic changes.

Cirsiliol represses proliferation of HCC through the PI3K signaling pathway

The CCK-8 assay demonstrated that the PI3K activator promoted the proliferation of endothelial cells after 24 hours of treatment, an effect counteracted by cirsiliol (**Figure 5A**, **5B**). Additionally, colony formation assays revealed that an ERK activator increased colony numbers, which were significantly reduced by subsequent cirsiliol treatment (**Figure 5C**).

Discussion

HCC represents the sixth most common cancer and the third leading cause of cancer-related mortality worldwide. It remains a significant public health challenge, with a shifting epidemiological landscape. Non-viral causes of liver disease have emerged as key risk factors for HCC, emphasizing the need for updated prevention and treatment strategies. In this study, we demonstrated that cirsiliol is a promising therapeutic agent for HCC. Cirsiliol treatment significantly suppressed HCC cell proliferation while inhibiting glutamine metabolism and reducing the production of glutamic acid and ATP.

Cancer is characterized by extensive metabolic reprogramming, with tumor cells often redirecting tricarboxylic acid (TCA) cycle precursors to synthesize nucleic acids, lipids, and proteins. This metabolic shift depletes TCA cycle intermediates and impairs mitochondrial function. To compensate, tumor cells adopt alternative strategies, including the enhanced utilization of glutamine [15, 16]. Glutamine is a pivotal metabolite that replenishes the TCA cycle through its conversion to α-ketoglutarate, providing energy and essential substrates for the synthesis of purines, pyrimidines, and the hexosamine pathway. Tumor cells' reliance on glutamine is critical for maintaining TCA cycle function, energy production, biomolecule synthesis, and redox homeostasis. For example, glutamine metabolism is essential for the viability of endometrial cancer cells [17]. Once transported into cells, glutamine is converted by gluta-

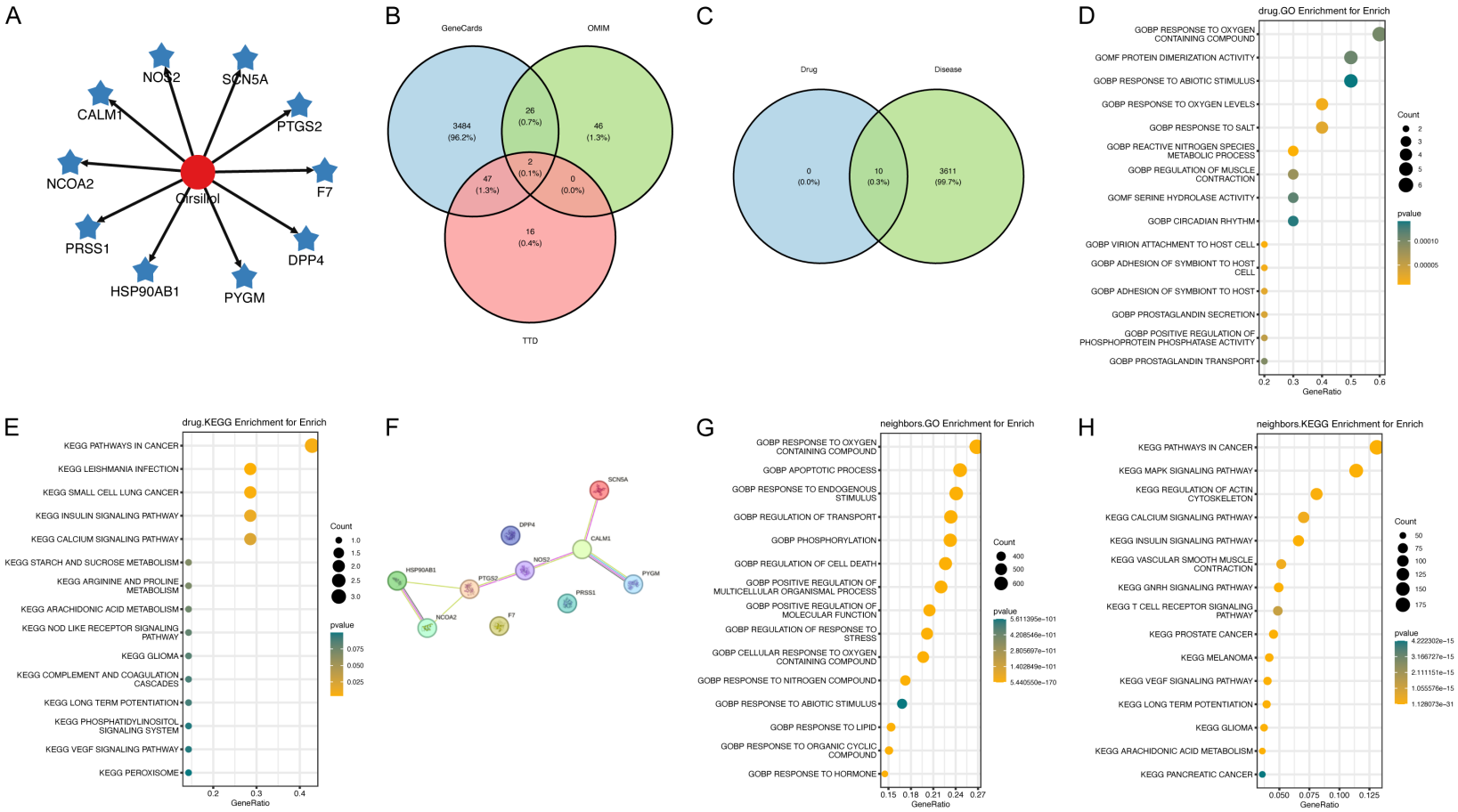

Figure 3. Network pharmacology analysis of potential signaling pathways targeted by cirsiliol in hepatocellular carcinoma. (A) The target genes of cirsiliol were screened using the TCMSP database. (B) Venn diagrams were constructed to map the target genes of HCC from Genecard, TTD and OMIM databases. (C) Venn diagrams were drawn to illustrate the intersection of standardized disease-associated targets with traditional Chinese medicine targets. (D) DO and (E) KEGG analysis of the 10 intersected genes. (F) PPI network of the 10 genes. (G) GO and (H) KEGG analysis of PPI network.

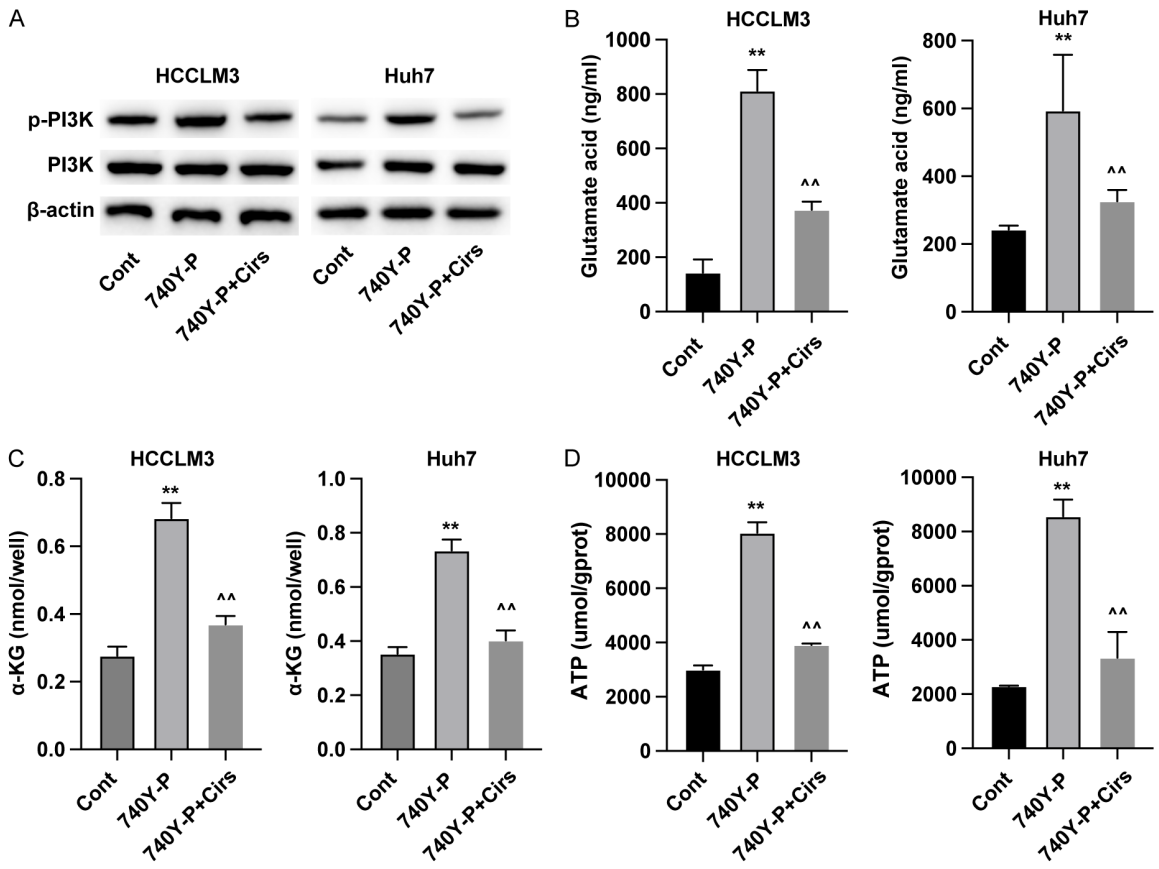

Figure 4. Cirsiliol modulates glutamine metabolism in hepatocellular carcinoma via the PI3K signaling pathway. A: Protein levels of total and phosphorylated PI3K were detected. B-D: The levels of glutamic acid, α-KG, and ATP in endothelial cells were measured. **P<0.05 vs cont, ^^P<0.05 vs 740Y-P.

minase (GLS) into glutamate and ammonia. Glutamate is subsequently transformed into α-ketoglutarate by glutamate dehydrogenase (GDH), fueling the TCA cycle [18].

In this study, we observed that cirsiliol treatment downregulated the phosphorylation of PI3K. Network pharmacological analysis also highlighted the role of metabolic pathways in cirsiliol-treated HCC cells. Previous research has shown that cirsiliol inhibits proliferation and induces apoptosis in various cancers [11-14], but its impact on cancer cell metabolism remains poorly understood. Our findings reveal, for the first time, that cirsiliol alters glutamine metabolism in HCC cells. Furthermore, we investigated the molecular mechanisms underlying this effect.

The PI3K signaling pathway is a key regulator of cancer cell metabolic reprogramming, particularly glutamine metabolism [19]. When activated, this pathway promotes glutamine uptake and utilization, which are critical for cancer cell proliferation and survival [20, 21]. The PI3K/Akt axis enhances the expression of glutamine transporters and glutaminase activity, driving glutamate production to fuel the TCA cycle and support the biosynthesis of nucleotides, lipids, and proteins [22]. Additionally, the PI3K pathway contributes to redox balance by regulating glutathione production, a vital antioxidant in cancer cells [23, 24]. Therefore, targeting the PI3K pathway could disrupt cancer-specific glutamine metabolism and serve as a therapeutic strategy. Previous studies have shown that cirsiliol modulates various signaling pathways, including PI3K/Akt, STAT3, and NF-κB, to inhibit cancer cell proliferation and metastasis [10, 12, 13].

In conclusion, our research demonstrates that cirsiliol effectively inhibits both the growth and glutamine metabolism of HCC cells. Further-

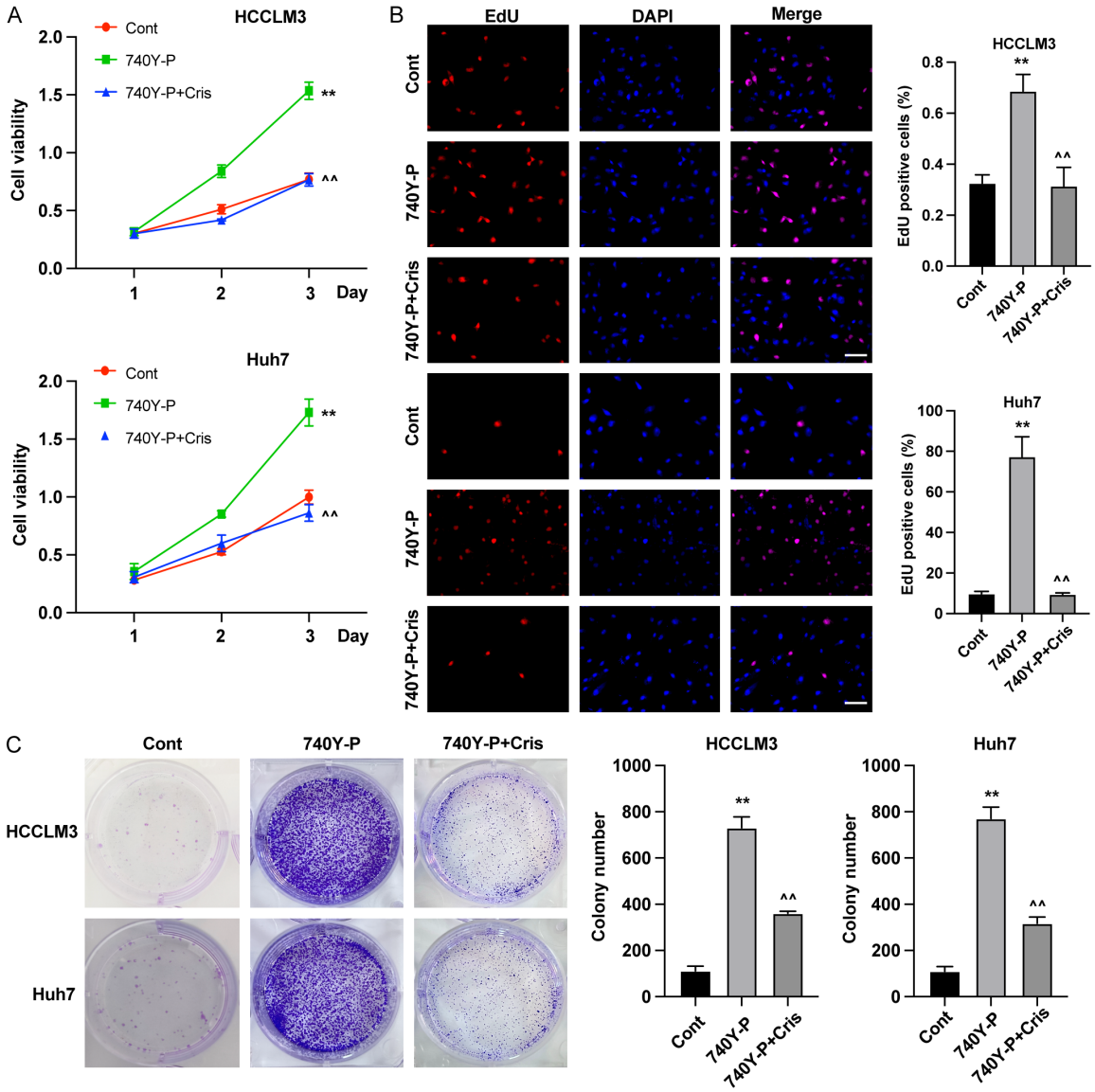

Figure 5. Cirsiliol restrains the proliferation of hepatocellular carcinoma through the PI3K signaling pathway. A: Cell viability was evaluated by CCK-8 assay. B: Cell proliferation was quantified by EdU assay. Scale bar: 20 μm. C: Cell proliferation was assessed by colony formation assay. **P<0.05 vs cont, ^^P<0.05 vs 740Y-P.

more, we identified the PI3K signaling pathway as a critical mediator of these effects. These findings provide new insights into the potential use of cirsiliol as a therapeutic agent for cancer treatment.

Acknowledgements

This study was supported by the Zhejiang Province Traditional Chinese Medicine Science and Technology Plan Funding Project (No. 2022ZB323); Zhejiang Province Medical and Health Science and Technology Plan Funding Project (No. 2022KY1114).

Disclosure of conflict of interest

None.

Address correspondence to: Siming Zheng, Hepatopancreatobiliary Surgery Department, The First Affiliated Hospital of Ningbo University, No. 59, Liuting Street, Haishu District, Ningbo 315000, Zhejiang, China. E-mail: zhengsiming1221@sina.com

References

[1] Park JH, Pyun WY and Park HW. Cancer metabolism: phenotype, signaling and therapeutic targets. Cells 2020; 9: 2308.

[2] Stine ZE, Schug ZT, Salvino JM and Dang CV. Targeting cancer metabolism in the era of precision oncology. Nat Rev Drug Discov 2022; 21: 141-162.
[3] Hay N. Reprogramming glucose metabolism in cancer: can it be exploited for cancer therapy? Nat Rev Cancer 2016; 16: 635-649.
[4] Mossmann D, Park S and Hall MN. mTOR signalling and cellular metabolism are mutual determinants in cancer. Nat Rev Cancer 2018; 18: 744-757.
[5] Zhu L, Zhu X and Wu Y. Effects of glucose metabolism, lipid metabolism, and glutamine metabolism on tumor microenvironment and clinical implications. Biomolecules 2022; 12: 580.
[6] Cluntun AA, Lukey MJ, Cerione RA and Locasale JW. Glutamine metabolism in cancer: understanding the heterogeneity. Trends Cancer 2017; 3: 169-180.
[7] Altman BJ, Stine ZE and Dang CV. From Krebs to clinic: glutamine metabolism to cancer therapy. Nat Rev Cancer 2016; 16: 619-634.
[8] Jin J, Byun JK, Choi YK and Park KG. Targeting glutamine metabolism as a therapeutic strategy for cancer. Exp Mol Med 2023; 55: 706-715.
[9] Yang WH, Qiu Y, Stamatatos O, Janowitz T and Lukey MJ. Enhancing the efficacy of glutamine metabolism inhibitors in cancer therapy. Trends Cancer 2021; 7: 790-804.
[10] Jiang T, Peng L, Wang Q, Huang B, Peng D, Men L, Jiang Y, Zhu M, Wang M, Lin L, Lv J and Li S. Cirsiliol regulates mitophagy in colon cancer cells via STAT3 signaling. Cancer Cell Int 2022; 22: 304.
[11] Kang J, Kim E, Kim W, Seong KM, Youn H, Kim JW, Kim J and Youn B. Rhamnetin and cirsiliol induce radiosensitization and inhibition of epithelial-mesenchymal transition (EMT) by miR-34a-mediated suppression of Notch-1 expression in non-small cell lung cancer cell lines. J Biol Chem 2013; 288: 27343-27357.
[12] Prasad P, Vasas A, Hohmann J, Bishayee A and Sinha D. Cirsiliol suppressed epithelial to mesenchymal transition in B16F10 malignant melanoma cells through alteration of the PI3K/Akt/NF-κB signaling pathway. Int J Mol Sci 2019; 20: 608.
[13] Luo M, Su Z, Gao H, Tan J, Liao R, Yang J and Lin L. Cirsiliol induces autophagy and mitochondrial apoptosis through the AKT/FOXO1 axis and influences methotrexate resistance in osteosarcoma. J Transl Med 2023; 21: 907.
[14] Jia X, Huang C, Hu Y, Wu Q, Liu F, Nie W, Chen H, Li X, Dong Z and Liu K. Cirsiliol targets tyrosine kinase 2 to inhibit esophageal squamous cell carcinoma growth in vitro and in vivo. J Exp Clin Cancer Res 2021; 40: 105.
[15] Jeong SM, Hwang S, Park K, Yang S and Seong RH. Enhanced mitochondrial glutamine anaplerosis suppresses pancreatic cancer growth through autophagy inhibition. Sci Rep 2016; 6: 30767.
[16] Owen OE, Kalhan SC and Hanson RW. The key role of anaplerosis and cataplerosis for citric acid cycle function. J Biol Chem 2002; 277: 30409-30412.
[17] Zhou WJ, Zhang J, Yang HL, Wu K, Xie F, Wu JN, Wang Y, Yao L, Zhuang Y, Xiang JD, Zhang AJ, He YY and Li MQ. Estrogen inhibits autophagy and promotes growth of endometrial cancer by promoting glutamine metabolism. Cell Commun Signal 2019; 17: 99.
[18] Still ER and Yuneva MO. Hopefully devoted to Q: targeting glutamine addiction in cancer. Br J Cancer 2017; 116: 1375-1381.
[19] Du D, Liu C, Qin M, Zhang X, Xi T, Yuan S, Hao H and Xiong J. Metabolic dysregulation and emerging therapeutical targets for hepatocellular carcinoma. Acta Pharm Sin B 2022; 12: 558-580.
[20] He Y, Sun MM, Zhang GG, Yang J, Chen KS, Xu WW and Li B. Targeting PI3K/Akt signal transduction for cancer therapy. Signal Transduct Target Ther 2021; 6: 425.
[21] Miricescu D, Totan A, Stanescu-Spinu II, Badoiu SC, Stefani C and Greabu M. PI3K/AKT/mTOR signaling pathway in breast cancer: from molecular landscape to clinical aspects. Int J Mol Sci 2020; 22: 173.
[22] Chakraborty S, Balan M, Sabarwal A, Choueiri TK and Pal S. Metabolic reprogramming in renal cancer: events of a metabolic disease. Biochim Biophys Acta Rev Cancer 2021; 1876: 188559.
[23] Duan F, Mei C, Yang L, Zheng J, Lu H, Xia Y, Hsu S, Liang H and Hong L. Vitamin K2 promotes PI3K/AKT/HIF-1α-mediated glycolysis that leads to AMPK-dependent autophagic cell death in bladder cancer cells. Sci Rep 2020; 10: 7714.
[24] Shiau JP, Chuang YT, Cheng YB, Tang JY, Hou MF, Yen CY and Chang HW. Impacts of oxidative stress and PI3K/AKT/mTOR on metabolism and the future direction of investigating fucoidan-modulated metabolism. Antioxidants (Basel) 2022; 11: 911.

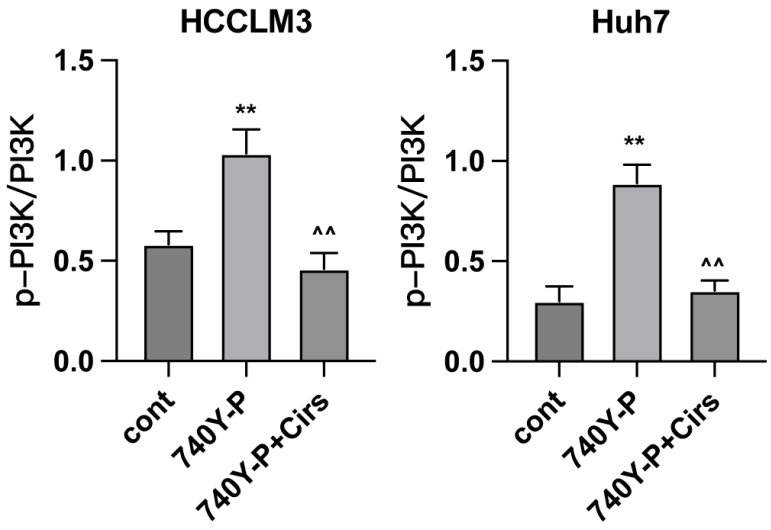

Figure S1. Quantification of phosphorylated PI3K level in HCCLM3 and Huh7 cells.